Deuterium NMR Study of Unstable Phenomena and Water Molecular Dynamics in Samarium Nitrate Hexahydrate Crystal

Motohiro Mizuno,* Yasuyuki Hamada, Tetsu Kitahara, and Masahiko Suhara

Department of Chemistry, Faculty of Science, Kanazawa University, Kanazawa 920-1192, Japan

Received: December 8, 1998

Deuterium NMR spectra, spin−lattice relaxation time T_1, and differential thermal analysis (DTA) were measured for $Sm(NO_3)_3 \cdot 6D_2O$. The magnetization recovery can be divided into two components. From deuterium NMR spectra and T_1, the short and the long components of T_1 were found to be mainly dominated by the 180° flip of the crystallization and the coordinated water molecules, respectively. For the nonannealed sample, the reproducibility of T_1 was observed. The influence of the instability was not seen in the long component of T_1. The results of the long component of T_1 gave the activation energy $E_a = 20$ kJ mol^{-1} and the correlation time at infinite temperature $\tau_{c0} = 7.8 \times 10^{-12}$ s for the 180° flip of the coordinated water molecule. The motion of the crystallization water at low temperatures can be explained by the 180° flip in the asymmetric double minimum potential. $\tau_{c0} = 1.2 \times 10^{-12}$ s, $E_a = 16$ kJ mol^{-1}, and the energy difference in the potential wells $\Delta E = 2.0$ kJ mol^{-1} were obtained for the 180° flip of the crystallization water from the short component of T_1. The potential wells for the 180° flip of the crystallization water changed gradually in phase II and approached the symmetric wells with increasing temperature. For the annealed sample, the drastic change of T_1 was observed in phases II and III. Both the long and the short components of T_1 did not show the reproducibility. These unstable phenomena are interpreted in terms of the metastable state due to the change of the hydrogen bond between the crystallization and the coordinated waters by annealing.

Introduction

Recently, the unstable phenomena of the electric and the magnetic properties have been reported for the several rare-earth nitrate crystals.[1−17] Samarium nitrate hexahydrate, $Sm(NO_3)_3 \cdot 6H_2O$, has been reported to have four phases.[1−7,18] In these phases, phase II exists in the temperature range from ca. 283 to 228 K and is known to be unstable. The temperature variation of the dielectric constant is accompanied by the large thermal hysteresis and is not reproducible in phase II.[1−7] These phenomena are different from the usual phase transition. Kawashima et al. have attempted to analyze the instability of phase II at the nonlinear and nonequilibrium properties.[1−17] However, the origin of the instability is not elucidated and it is interesting to study the static and the dynamic structure of this crystal. The symmetry of $Sm(NO_3)_3 \cdot 6H_2O$ is triclinic and the space group is $P\bar{1}$ at room temperature.[19,20] For six water molecules, four coordinated waters are directly coordinated to the metal, whereas two crystallization waters do not. From the investigation of ^{1}H NMR spin−lattice relaxation time T_1, spin−lattice relaxation time in rotating frame $T_{1\rho}$, and doped Gd^{3+} ESR spectra, we have shown that the motion of the water molecules, especially the crystallization water molecules, plays an important role in the unstable state.[18] Since the crystallization waters form only one O−H···O hydrogen bond, the 180° flip of the water molecules is predicted to occur in the unequal double minimum potential. The variation of these potential wells is considered to be related to the phase transition and the instability. Deuterium NMR is effective for studying the environment and motion of water molecules. The nuclear quadrupole interaction parameters are sensitive for the environment of the water molecule. The information for the motion of the water molecule can be obtained by the deuterium NMR spectral simulation and T_1.[21−25] The nuclear quadrupole coupling constant e^2Qq/h, asymmetry parameter η and the jumping rate of the water molecule in the paramagnetic $Sm(NO_3)_3 \cdot 6D_2O$ can be obtained from the deuterium NMR spectra and T_1 by using the shift-compensated pulse sequence which refocuses both the quadrupole interaction and the paramagnetic shift.[25−31] In the present paper, for the purpose of clarifying the mechanism of the instability in $Sm(NO_3)_3 \cdot 6H_2O$, deuterium NMR spectra and T_1 were measured and the behavior of the water molecules were discussed. The effect of annealing was studied by keeping the sample at 340 K for 1 h. The crystallization waters that were fixed by the hydrogen bond from the coordinated waters and nitrate ion[19,20] became free at this temperature. The change of the hydrogen bonds surrounding the crystallization waters by annealing is presumed to alter the properties of $Sm(NO_3)_3 \cdot 6D_2O$.

Experimental Section

The deuterated sample was prepared by repeated recrystallization from heavy water. ^{2}H NMR was measured by a CMX-300 spectrometer at 45.835 MHz. The $(\pi/2)_x-\tau/2-(\pi)_y-\tau/2-(\pi/2)_y-\tau/2-(\pi)_y-\tau/2-$acq pulse sequence was used, which refocuses the dephasing due to the quadrupole interaction and the paramagnetic shift.[25−27,31] $\pi/2$ pulse width and $\tau/2$ were 2.0 and 20 μs, respectively. ^{2}H NMR T_1 was measured by the inversion recovery method. The magnetization recovery was observed by using the integrated intensity of the spectrum. The DTA measurement was performed by a homemade apparatus.

Results and Discussion

DTA. The DTA measurement was repeated between 140 and 330 K. Two heat anomalies were detected at 192 and 245 K in

* Corresponding author. Reprint requests to Dr. M. Mizuno. E-mail: mizuno@wriron1.s.kanazawa-u.ac.jp.

10.1021/jp984664v CCC: $18.00
Published on Web 06/16/1999

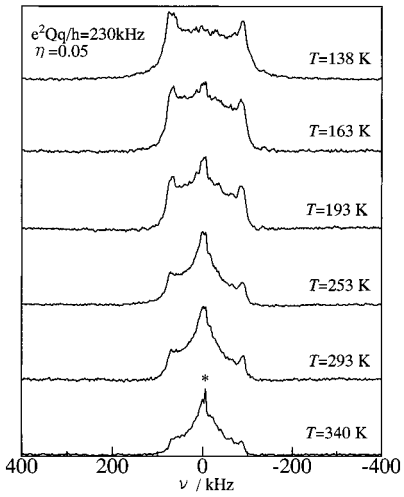

Figure 1. Observed ^{2}H NMR spectra for $Sm(NO_3)_3 \cdot 6D_2O$ using the shift-compensated pulse sequence. The asterisk shows the sharp component of the spectrum arises from free D_2O.

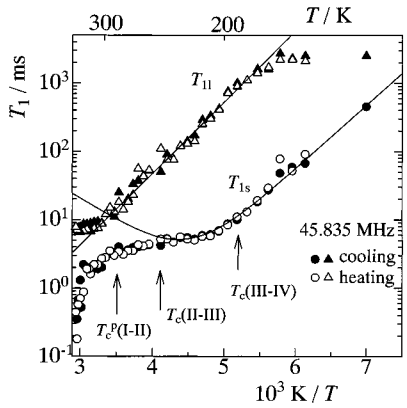

Figure 2. Temperature dependence of ^{2}H NMR T_1 in $Sm(NO_3)_3 \cdot 6D_2O$. (●) and (○) show T_{1s} in the cooling and heating processes, respectively. (▲) and (△) show T_{1l} in the cooling and heating processes, respectively. T_c(II−III) and T_c(III−IV) show the transition temperature determined by the present DTA measurement. T_c^p(I−II) shows the phase I−II transition point for the protonated compound. The solid lines show the theoretical curve for the 180° flip of the water molecule.

the heating process. In the cooling process, heat anomalies were detected at 229 and 181 K. The anomalies at 245 K in heating and 229 K in cooling are considered to correspond to the phase II−III transition observed by the dielectric constant and DTA for the protonated compound.[1−7,18] The anomalies at 192 K in heating and 181 K in cooling are considered to correspond to the phase III−IV transition observed by DTA for the protonated compound.[18] The phase II−III and III−IV transition points shifted to high temperature by ca. 5 and 9 K on deuteration, respectively. Although another anomaly of the dielectric constant has been reported around 283 K,[1−7] the heat anomaly was not detected in the present DTA investigation. The shift of the transition temperature was not observed on repeating runs.

^{2}H NMR. Spectra and T_1 for Nonannealed Sample. Figure 1 shows the temperature dependence of ^{2}H NMR spectra. The spectrum at 138 K showed the line shape due almost to the rigid D_2O. The asymmetry of the spectrum indicates that the paramagnetic shift caused by Sm^{3+} ions contributes to the spectrum.[25−27,31] The quadrupole coupling constant $e^2Qq/h = 230 \pm 2$ kHz and the asymmetry parameter $\eta = 0.05$ were estimated from the spectrum at 138 K. The central portion of the spectrum increased with increasing temperature and the spectrum with a large η value was obtained at high temperatures. These variations of the spectrum can be explained by the 180° flip of the water molecule.[24,25,27,31] The sharp component was observed in the center of the spectrum at 340 K. Prior to the melting point (346 K for the protonated compound), part of the water molecules become free.

Figure 2 shows the temperature dependence of ^{2}H NMR T_1. Since the magnetization recovery showed two components, the existence of two kinds of water molecules is recognized. The T_1 values for two components were estimated by using the integrated intensity in the entire area of the spectrum and analyzing mathematically in terms of two-component relaxation. The long and the short components of T_1 were denoted by T_{1l} and T_{1s}, respectively. The errors of T_{1l} and T_{1s} estimations were within ±10%. The temperature dependences of T_{1l} and T_{1s} were observed for three independently prepared samples. Both of T_{1l} and T_{1s} were reproducible to ±15%. We took into account the T_{1l} and T_{1s} errors of ±15% in the following discussion. Although T_{1s} decreased rapidly prior to the melting point, T_{1l} did not show such a phenomenon. Two crystallization waters, which are not directly coordinated to the metal, are predicted to become free at a lower temperature compared with four coordinated waters for six water molecules of $Sm(NO_3)_3 \cdot 6H_2O$.[19,20] This suggests that T_{1s} and T_{1l} are dominated by the crystallization and the coordinated waters, respectively. Below 180 K, T_{1l} decreased gently with decreasing temperature. T_{1l} is considered to be determined by the magnetic interaction between the ^{2}H nucleus and Sm^{3+} ions.[18] Between 180 and 283 K, T_{1l} is considered to be dominated by the 180° flip of the coordinated water molecule, since T_{1l} decreased exponentially with increasing temperature. The temperature dependence of T_{1l} showed the correlation time τ_c for the 180° flip of the water molecule, which satisfied the slow-motion condition $\omega_0\tau_c \gg 1$, where ω_0 is the angular NMR frequency. Assuming $\eta = 0$, T_{1l} can be written as[21−23]

$$T_{1l}^{-1} = \frac{1}{5}\left(\frac{\omega_Q}{\omega_0}\right)^2 \frac{1}{\tau_c} \sin^2(2\beta) \quad (1)$$

$$\omega_Q = \frac{3e^2Qq}{4\hbar} \quad (2)$$

where 2β is the D−O−D angle of the water molecule. Assuming an Arrhenius-type relationship, τ_c is given by

$$\tau_c = \tau_{c0} \exp\left(\frac{E_a}{RT}\right) \quad (3)$$

where τ_{c0} and E_a are the correlation time at infinite temperature and the activation energy for the 180° flip of the water molecule. The fitting calculation was performed using $e^2Qq/h = 230$ kHz and $2\beta = 110°$, which were estimated by the ^{2}H NMR spectrum at 138 K and the crystal structure.[19] $\tau_{c0} = 7.8 \times 10^{-12}$ s and $E_a = 20 \pm 3$ kJ mol^{-1} for the coordinated water were obtained from the fitting. Above ca. 283 K (the phase I−II transition point for the protonated compound), T_{1l} deviated from the temperature dependence at low temperatures. This means that the environment of the coordinated water changes around this temperature. In phases III and IV, T_{1s} decreased exponentially with increasing temperature at low temperatures and showed a shallow minimum at ca. 220 K. The observed minimum value of T_{1s} (ca. 5 ms) is larger than 2.0 ms, which was predicted by the 180° flip of the water molecule between the symmetric potential wells and $e^2Qq/h = 230$ kHz. This shallow minimum of T_{1s} can be explained by the 180° flip of the water molecule in the asymmetric double minimum potential, as shown in Figure 3a.[32,33] These potential wells are consistent with the local

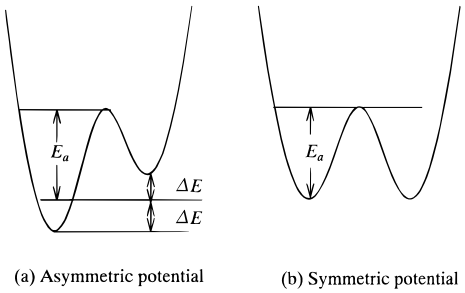

Figure 3. Potentials for the 180° flip of the water molecule in $Sm(NO_3)_3 \cdot 6D_2O$. (a) and (b) show the asymmetric and symmetric double minimum potential, respectively.

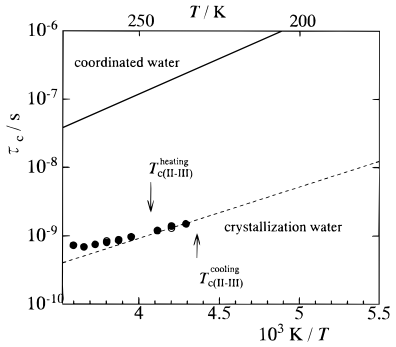

Figure 4. Correlation times τ_c of the 180° flip for two kinds of water molecules in $Sm(NO_3)_3 \cdot 6D_2O$. The solid line shows τ_c for the coordinated water molecule obtained by the fitting calculation of T_{1l}. The broken line shows τ_c for the crystallization water molecule obtained by the fitting calculation of T_{1s} in phases III and IV. (●) and (○) show τ_c obtained by T_{1s} in phase II. The arrows indicate the phase II−III transition point determined by DTA in the heating and cooling processes.

structure of the crystallization waters that form only one O−D···O hydrogen bond.[19] T_{1s} is written by assuming $\eta = 0$ as[32,33]

$$T_{1s}^{-1} = \frac{1}{10}\frac{a}{(1+a)^2}\left(\frac{3e^2Qq}{4\hbar}\right)^2 \times (\sin 2\beta)^2\left\{\frac{\tau_c}{1+\omega_0^2\tau_c^2} + \frac{4\tau_c}{1+4\omega_0^2\tau_c^2}\right\} \quad (4)$$

$$a = \exp\left(\frac{2\Delta E}{RT}\right) \quad (5)$$

$$\tau_c = (1+a)^{-1}\tau_{c0}\exp\left(\frac{E_a + \Delta E}{RT}\right) \quad (6)$$

The fitting calculation was performed with τ_{c0}, E_a, and the deviation from the symmetric potential wells ΔE as parameters. $e^2Qq/h = 230$ kHz and $2\beta = 110°$ were used. The fitting curve was shown by the solid line in Figure 2. $\tau_{c0} = 1.2 \times 10^{-12}$ s, $E_a = 16 \pm 2$ kJ mol^{-1}, and $\Delta E = 2.0 \pm 0.3$ kJ mol^{-1} were obtained by the fitting. T_{1s} in phase II deviated from the temperature dependence in phases III and IV and decreased gradually with increasing temperature. The temperature dependence of T_{1s} in phase II can be explained by the change of the potential for the 180° flip of the crystallization water molecule.[32] In phase II, the asymmetric potential wells for the 180° flip of the crystallization water molecule as Figure 3a can be considered to gradually approach the symmetric wells in Figure 3b with increasing temperature. ΔE and τ_c were estimated from the T_{1s} values in phase II using eqs 4−6 with $\tau_{c0} = 1.2 \times 10^{-12}$ s, $E_a = 16$ kJ mol^{-1}, $e^2Qq/h = 230$ kHz, and $2\beta = 110°$. Figure 4 shows the temperature dependence of τ_c. In phase II, τ_c for the

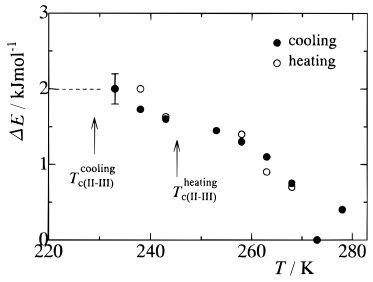

Figure 5. Temperature variation of the energy difference ΔE in the asymmetric double minimum potential for the 180° flip of the crystallization water molecule in $Sm(NO_3)_3 \cdot 6D_2O$. (●) and (○) show ΔE in the cooling and heating process, respectively. The arrows indicate the phase II−III transition point determined by DTA in the heating and cooling processes.

180° flip of the crystallization water deviated from the temperature dependence shown in phases III and IV. Figure 5 shows the temperature variation of ΔE. The error of ΔE was estimated as ±15% (error bar in Figure 5), which was mainly caused by the accuracy of T_{1s}. The ΔE value for the 180° flip of the crystallization water molecule decreased gradually with increasing temperature and reached zero at ca. 283 K. This variation of the potential is considered to be related closely to the instability in phase II. Above ca. 283 K, another contribution to the relaxation of the ^{2}H nucleus, other than the 180° flip of the water molecule, is considered to exist, since T_{1s} decreased further with increasing temperature.

The spectral simulation was performed in order to clarify the behavior and the proportion of the coordinated and the crystallization waters.

The jumping rate k for the 180° flip of the water molecule is written as

$$k = (2\tau_c)^{-1} \quad (7)$$

Using eq 7, the k values of the coordinated and the crystallization waters were estimated from τ_c obtained by T_{1l} and T_{1s}, respectively. Parts a and b of Figure 6 are the ^{2}H NMR spectral simulations for the coordinated and the crystallization water molecules, respectively. The solid lines in Figure 6c show the observed spectra. As shown by the broken lines in Figure 6c, the observed spectra could be interpreted by the combination of the simulated spectra for two kinds of water molecules (Figure 6a,b) in the ratio (a)/(b) = 2. Although the ratio was poorly determined at 253 K, the accuracy of the ratio was within ±0.5 at other temperatures. Since the ratio of the coordinated and the crystallization waters has been reported as 2:1,[19,20] the assignment of the water molecules to T_{1l} and T_{1s} is considered to be proper. Good agreement between the observed and the simulated spectra suggests that the motional parameters of the water molecules (τ_{c0}, E_a, and ΔE) obtained from ^{2}H NMR T_1 are reasonable.

***T*$_1$ for Annealed Sample.** Figure 7 shows the temperature dependence of ^{2}H NMR T_1 for the sample annealed at 340 K for one hour. In phase IV, T_{1s} and T_{1l} showed reproducibility within ±15% on repeating runs. In phases II and III, however, both T_{1s} and T_{1l} changed largely and did not show the reproducibility. The similar change of the properties due to the annealing has been reported from the measurements of the dielectric constant.[1−17] The crystallization and coordinated waters are predicted to be in the unstable state by annealing. The minimum value of T_{1s} around 220 K changed for each run, which suggests that the potential for the 180° flip of the crystallization waters changes on repeating runs. The crystal-

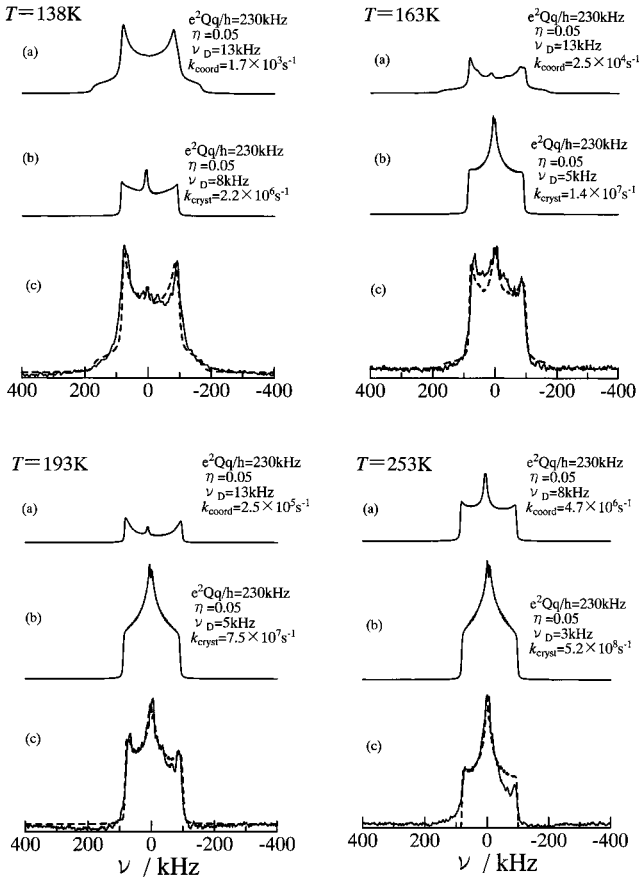

Figure 6. Observed and theoretical ^{2}H NMR spectra for $Sm(NO_3)_3 \cdot 6D_2O$. (a) The theoretical spectra for the coordinated water molecule. (b) The theoretical spectra for the crystallization water molecule. (c) The solid lines show the observed spectra. The broken lines show the theoretical spectra obtained by the combination of (a) and (b) in the ratio 2:1.

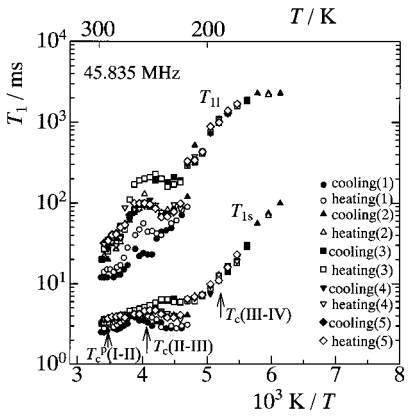

Figure 7. Temperature dependence of ^{2}H NMR T_1 for annealed $Sm(NO_3)_3 \cdot 6D_2O$ in several measuring runs of cooling and heating. T_c(II−III) and T_c(III−IV) show the transition temperature determined by the present DTA measurement. T_c^p(I−II) shows the phase I−II transition point for the protonated compound.

lization waters are fixed by the hydrogen bond from the coordinated waters and the nitrate ion.[19,20] The sharp component of the ^{2}H NMR spectrum at 340 K reveals that these hydrogen bonds were broken and a part of crystallization waters became free. It is thought that a manner of the hydrogen bonds was varied by annealing and the unstable state took place. The temperature variation of ΔE for the crystallization water in the nonannealed sample suggests that the site of the crystallization water is somewhat less stable at high temperatures. Therefore,

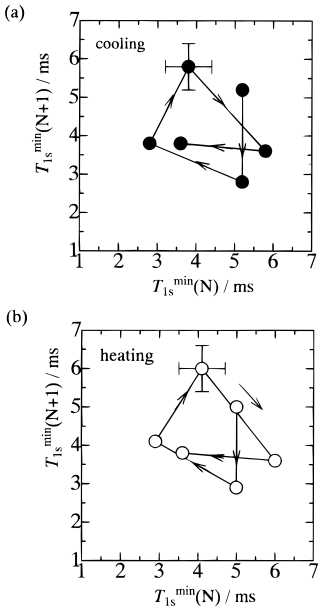

Figure 8. Return maps for the minimum values of ^{2}H NMR T_{1s} for annealed $Sm(NO_3)_3 \cdot 6D_2O$. The minimum values of T_{1s} at the $(N+1)$th run are plotted as the ordinate and at the Nth run as the abscissa. (a) and (b) show the results of the cooling and heating processes, respectively.

a part of the crystallization waters may enter the interstitial positions around the regular site after annealing. If these waters change the site or the orientation easily near room temperature, the potential of the 180° flip will be altered on a repeating run. Figure 8 shows the return map that is plotted with the minimum values of T_{1s} at the $(N+1)$th run as the ordinate and at the Nth run as the abscissa. The error of ±15% represented in Figure 8 was estimated from the accuracy of T_{1s} for the annealed sample in phases IV and the nonannealed sample. The return map showed the spiral pattern as seen in the dielectric constant.[3,4] If the minimum of T_{1s} changes at random, any regularity cannot be seen in this map. Therefore, the correlation between each run is considered to exist. The memory effect observed in the present work is predicted to be related closely to the hydrogen bond network surrounding the crystallization waters.

Conclusion

The existence of two kinds of waters was confirmed from ^{2}H NMR T_1. The results of the ^{2}H NMR spectra and T_1 suggest that one is the crystallization water that dominates the short component of T_1; another is the coordinated water that dominates the long component of T_1. The potential wells for the 180° flip of the crystallization water changed gradually in phase II. For the annealed sample, the unstable behavior of T_1, which did not show reproducibility, reveals that a manner of hydrogen bond of the crystallization water varied and the metastable state arised by annealing. The variation of the environment of the crystallization water is considered to affect the motion of the coordinated water and causes the large change of the long component of T_1. From the return map for the minimum values of the short component of T_1, the existence of regularity in the change of the potential for the 180° flip of the crystallization water on repeating run was predicted. The hydrogen bonds surrounding the crystallization waters are considered to play an important role in the memory effect revealed in the present results of ^{2}H NMR.

Appendix: Spectral Simulation

In the following we describe the simulation of the ^2H NMR spectrum for the paramagnetic $Sm(NO_3)_3 \cdot 6D_2O$. The nuclear quadrupole interaction and the electron-nuclear dipolar interaction between the ^2H nuclei and Sm^{3+} ions are considered to contribute mainly to the spectra. The spectral simulation was performed by using the model of two-site 180° flips of the water molecules about the D−O−D bisector, which is assumed to be parallel to the Sm−O direction. For the $^2H-Sm^{3+}$ dipolar interaction, the contribution from the nearest Sm^{3+} ion ($\omega_D = 2\pi\nu_D$) was estimated. On the assumption of the isotropic **g** tensor, the site frequency ω_i is written by the second-order Wigner rotation matrix $D^{(2)*}_{nm}(\Omega)$ as[24,25,31,34]

$$\omega_i = \mp\omega_Q - \omega_P \tag{A1}$$

$$\omega_Q = (3/2)^{1/2} \sum_{n,m=-2}^{2} D^{(2)*}_{0n}(\psi,\theta,\phi) D^{(2)*}_{nm}(\alpha,\beta,\gamma)\, T^{(2)}_{mQ} \tag{A2}$$

$$\omega_P = \sum_{n=-2}^{2} D^{(2)*}_{0n}(\psi,\theta,\phi)\, D^{(2)*}_{n0}(\alpha',\beta',\gamma')\, \omega_D \tag{A3}$$

$$T^{(2)}_{0Q} = (3/8)^{1/2} e^2Qq/\hbar \qquad T^{(2)}_{\pm 2Q} = (\eta/4) e^2Qq/\hbar \tag{A4}$$

$$\omega_D = 2\gamma_D g \mu_B \langle \mathbf{S}_z \rangle r^{-3} \tag{A5}$$

where, (α,β,γ), (ψ,θ,ϕ), and (α',β',γ') represent the Euler angles for the transformation from the molecular axes to the principal axis system of the quadrupolar tensor, from the laboratory axes to the molecular axes, and from the molecular axes to the principal axis system of the dipolar tensor between the ^2H nuclei and the nearest Sm^{3+} ion, respectively. $\langle \mathbf{S}_z \rangle$ is the expectation value for $\mathbf{S}_z$ of the unpaired electron spin in the Sm^{3+} ion. γ_D is the gyromagnetic ratio of the ^2H nucleus, and μ_B is the Bohr magneton. r is the distance between the ^2H nucleus and Sm^{3+} ion. The frequencies of ^2H in the two sites (ω_1, ω_2) were specified by $\alpha = \alpha' = 0$ and π. The angles between the rotation axis and the quadrupole principal axis are $\beta = 55°$. Between the rotation axis and Sm−D vector $\beta' = 15°$ and $\gamma = 0$ were used.[25,27] For the case of the infinitesimal short radio-frequency pulse widths, the signal collected beginning at the top of the resulting echo $G(t,\theta,\phi)$ is written as[24,25,31]

$$G(t,\theta,\phi) = \mathbf{P} \cdot \exp[\hat{\mathbf{A}}t] \exp(\hat{\mathbf{A}}\tau) \exp(\hat{\mathbf{A}}^*\tau) \cdot \mathbf{1} \tag{A6}$$

$$\hat{\mathbf{A}} = \begin{pmatrix} i\omega_1 - k & k \\ k & i\omega_2 - k \end{pmatrix} \tag{A7}$$

Here, **1** is a vector written by $\mathbf{1} = (1, 1)$. A vector of site populations was assumed as $\mathbf{P} = (1/2, 1/2)$. The effect of finite $\pi/2$ pulse widths was taken into account for $G(t,\theta,\phi)$ based on ref 35. The signal of the powder sample $G(t)$ is given by

$$G(t) = \int_0^{2\pi} \int_0^{\pi} G(t,\theta,\phi) \sin\theta \, d\theta \, d\phi \tag{A8}$$

The spectrum was obtained by the Fourier transform of $G(t)$.

References and Notes

(1) Kawashima, R.; Matsuda, T. *Phys. Stat. Sol. (a)* **1988**, *108*, K73.
(2) Kawashima, R. *J. Phys. Soc. Jpn.* **1987**, *56*, 415.
(3) Kawashima, R.; Matsuda, T. *J. Phys. Soc. Jpn.* **1989**, *58*, 3435.
(4) Kawashima, R.; Matsuda, T. *J. Phys. Soc. Jpn.* **1990**, *59*, 3727.
(5) Kawashima, R.; Nishimura, S.; Isoda, H. *Physica* **1993**, *B183*, 135.
(6) Kawashima, R.; Nishimura, S.; Isoda, H. *Physica* **1994**, *B203*, 59.
(7) Kawashima, R.; Isoda, H. *J. Phys. Soc. Jpn.* **1996**, *65*, 1133.
(8) Kawashima, R. *Solid State Commun.* **1989**, *70*, 393.
(9) Kawashima, R. *Solid State Commun.* **1991**, *78*, 553.
(10) Kawashima, R.; Isoda, H. *J. Phys. Soc. Jpn.* **1990**, *59*, 3408.
(11) Kawashima, R.; Hattori, M. *J. Phys. Soc. Jpn.* **1992**, *61*, 1427.
(12) Kawashima, R.; Nasukawa, S.; Isoda, H. *J. Solid State Chem.* **1993**, *107*, 503.
(13) Kawashima, R.; Saitoh, T.; Isoda, H. *J. Phys. Soc. Jpn.* **1993**, *62*, 4529.
(14) Kawashima, R.; Hattori, M.; Isoda, H. *J. Phys. Chem. Solids* **1994**, *55*, 1331.
(15) Kawashima, R.; Fukase, T.; Isoda, H. *J. Phys. Chem. Solids* **1996**, *57*, 539.
(16) Kawashima, R.; Isoda, H. *Phys. Stat. Sol. (a)* **1996**, *153*, 501.
(17) Kawashima, R.; Kawasaki, M.; Isoda, H. *Chaos, Solitons Fractals* **1996**, *7*, 1863.
(18) Mizuno, M.; Ito, E.; Suhara, M. *J. Phys. Chem. Solids* **1999**, *60*, 195.
(19) Rogers, D. J.; Taylor, N. J.; Toogood, G. E. *Acta Crystallogr.* **1983**, *C39*, 939.
(20) Gshneider, K. A., Jr.; Eyring, L. *Handbook on the Physics and Chemistry of Rare Earths*; North-Holland Publishing Co.: Amsterdam, 1986; Vol. 8, p 302.
(21) Hiyama, Y.; Silverton, J. V.; Torchia, D. A.; Gerig, J. T.; Hammond, S. J. *J. Am. Chem. Soc.* **1986**, *108*, 2715.
(22) Torchia, D. A.; Szabo, A. *J. Magn. Reson.* **1982**, *49*, 107.
(23) Vold, R. R.; Vold, R. L. *Advances in Magnetic and Optical Resonance*; Warren, W. S., Ed.; Academic Press, Inc.: New York, 1991; Vol. 16.
(24) Greenfield, M. S.; Ronemus, A. D.; Vold, R. L.; Vold, R. R.; Ellis, P. D.; Raidy, T. E. *J. Magn. Reson.* **1987**, *72*, 89.
(25) Vold, R. R. *Nuclear Magnetic Resonance Probes of Molecular Dynamics*; Tycko, R., Ed.; Kluwer Academic Publishers: Netherlands, 1994; p 27.
(26) Shiminovitch, D. J.; Rance, M.; Jeffrey, K. R.; Brown, M. F. *J. Magn. Reson.* **1984**, *58*, 62.
(27) Lin, T. -H.; DiNatale, J. A.; Vold, R. R. *J. Am. Chem. Soc.* **1994**, *116*, 2133.
(28) Woehler, S. E.; Wittebort, R. J.; Oh, S. M.; Hendrickson, D. N.; Inniss, D.; Strouse, C. E. *J. Am. Chem. Soc.* **1986**, *108*, 2938.
(29) Woehler, S. E.; Wittebort, R. J.; Oh, S. M.; Kambara, T.; Hendrickson, D. N.; Inniss, D.; Strouse, C. E. *J. Am. Chem. Soc.* **1987**, *109*, 1063.
(30) Oh, S. M.; Wilson, S. R.; Hendrickson, D. N.; Woehler, S. E.; Wittebort, R. J.; Inniss, D.; Strouse, C. E. *J. Am. Chem. Soc.* **1987**, *109*, 1073.
(31) Iijima, T.; Mizuno, M.; Suhara, M. *Z. Naturforsch.* **1998**, *53A*, 447.
(32) Morimoto, K.; Shimomura, K.; Yoshida, M. *J. Phys. Soc. Jpn.* **1983**, *52*, 3927.
(33) Look, D. C.; Lowe, I. J. *J. Chem. Phys.* **1966**, *44*, 3437.
(34) Rose, M. E. *Elementary Theory of Angular Momentum*; Wiley: New York, 1957.
(35) Barbara, T. M.; Greenfield, M. S.; Vold, R. L.; Vold, R. R. *J. Magn. Reson.* **1986**, *69*, 311.